3.4 CLOUD RADIATIVE FORCING IN ARCTIC POLYNYAS: CLIMATOLOGY, PARAMETERIZATION, AND MODELING

Erica L. Key *, Peter J. Minnett, Robert H. Evans
University of Miami, Rosenstiel School of Marine and Atmospheric Science, Miami, Florida

Tim N. Papakyriakou
University of Manitoba, Centre for Earth Observation Studies, Winnipeg, Manitoba

1. INTRODUCTION

Although the complex structure, relative ubiquity, and importance of Arctic clouds to the global climate system have been documented in numerous papers (e.g. Curry et al, 1996; Hobbs et al, 2001), so too have the difficulties polar environments pose to in situ and satellite retrieval of cloud and cloud properties (e.g. Schweiger and Key, 1992; Han and Stamnes, 1999; Maslanik et al, 2001). It is this latter constraint on measuring polar clouds which introduces uncertainties into radiative transfer models, and thus into calculations of surface radiative forcing. Currently available validating measurements are spatio-temporally limited and often concentrated in coastal areas conveniently accessible to icebreakers and aircraft surveys. Previous sensitivity studies have attributed O10 $W \cdot m^{-2}$ error in surface radiative fluxes to microphysical uncertainties (Curry et al, 1993) and incorrect cloud classification (Schweiger and Key, 1992; Chen et al, 2000). Only by merging high resolution data from a variety of platforms over a wide range of conditions, such as those found in the microcosms of Arctic polynyas, can we hope to accurately resolve the inherent variability of the polar atmosphere as well as the role of cloud cover in shaping the cryosphere and greater climate system.

2. DATA AND METHODOLOGY

Data collected within four Arctic polynyas over the past decade are used to evaluate current climatological conditions and determine how data uncertainties and losses impact the parameterization and modeling of the surface radiative flux. Each of these polynya data sets includes surface and atmospheric profile measurements collected aboard icebreakers, from coastal weather stations and project sites, as well as remotely-sensed scenes. The study areas span from east to west (Figure 1), Northeast Water Polynya (NEW) on the northeastern coast of Greenland; the North Water Polynya (NOW) between Ellesmere Island and Greenland; the Beaufort Flaw Lead (BFL) which parallels the North Slope of Alaska (NSA); and the shallow St. Lawrence Island Polynya (SLIP) in the Bering Sea. Despite climatic importance of these ice-free areas, no regional impact study has yet been performed.

2.1 CLIMATOLOGY

Past Arctic cloud observations include ship-based (Warren et al, 1988), land-based (Huschke, 1969), and satellite-derived model output (Rossow et al, 1991).

In this study, recent measurements from all three source types are categorized, processed, and modeled. Cloud form, areal coverage, and relative sun-cloud position were determined by a meteorologist analyzing time-lapse images of hemispheric sky cover collected both aboard ship and at the ARM (Atmospheric Radiation Measurement) Program's NSA site. By having the same observer classify all images and comparing each frame against concurrent AVHRR cloud masks and SeaWiFS visible imagery, both multiple observer and view angle bias were minimized in the classification process. Similar multi-platform techniques were used to estimate cloud-top temperature and cloud thickness, which were initially derived from radiosonde profiles, then tuned with co-located AVHRR and TOVS retrievals.

Other cloud microphysical parameters, such as particle radius and ice/liquid water path have only recently been made available by radar-lidar arrays at the SHEBA (Surface Heat Budget of the Arctic) and ARM/NSA sites, both located in the Beaufort Sea region. Coincidentally, prior aircraft surveys, which constitute the bulk of in situ microphysical data, were conducted along the Beaufort Sea coast. Consequently, the average microphysical structure is biased towards this coastal plain environment, one influenced by seasonal intrusions of pollution and Arctic Haze not present in any of the other three polynya areas. It is assumed because of this, and because most aircraft studies sampled in early spring during high particle concentration, that the average particle

radius is negatively skewed, thereby positively influencing the liquid droplet concentration and reflectivity of the cloud.

2.2 PARAMETERIZATION

To determine the sign of cloud radiative forcing at the surface, the Ramanathan et al, (1989) definition is used:

$C_{net} = C_{SW} + C_{LW}$

where $C_{SW} = SW\downarrow_{(c)} - SW\downarrow_{(0)}$

and $C_{LW} = LW\downarrow_{(c)} - LW\downarrow_{(0)}$.

Negative values of C_{net} indicate a preference for scattering and attenuation over longwave emission at the cloud base, such that clouds serve to cool the surface. Under observed cloudy-sky conditions ($SW\downarrow_{(c)}$, $LW\downarrow_{(c)}$) the theoretical clear-sky radiation ($SW\downarrow_{(0)}$, $LW\downarrow_{(0)}$) must be parameterized, often using simple radiative relationships.

Four shortwave and nine longwave clear-sky downwelling parameterizations were chosen from the literature for their applicability to Arctic marine and coastal environments. The only measured quantities required by these parameterizations are surface air temperature, *T*, and vapor pressure, *e*. The transmissivity parameter, *k*, is also data-derived, as it is dependent on the ratio of TOA (top-of-the-atmosphere) downwelling shortwave radiation to incident surface insolation scaled by the cosine of the solar zenith angle (Minnett, 1999). Remaining solar geometry and TOA variables were calculated from time and position data. Final assessment of parameterization performance was made by identifying those shortwave and longwave equations which incurred the lowest RMS uncertainty for each polynya data set and field season.

2.3 RADIATIVE TRANSFER MODELING

In order to explore the relationship between surface cloud forcing and a varying polar atmosphere, a radiative transfer model, Streamer (Key and Schweiger, 1998), was initialized with radiosonde and profile data. After sensitivity runs in which model-prescribed profiles of aerosol and ozone and a wide assortment of surface types were tested, remote sensing, ozonesonde, lidar, and radar data were assimilated to approximate realistic conditions for each radiosonde launch.

3. RESULTS AND CONCLUSIONS

In agreement with previous studies by Curry and Ebert (1992), cloudy skies accounted for 80% or more of the summertime atmosphere in all four polynyas sampled. Stratiform (stratus and altostratus) and cumuliform (cumulus, altocumulus, and stratocumulus) clouds outnumbered cirriform (cirrus, cirrostratus, and cirrocumulus), though occurrences of multiple cloud types accounted for one-fifth of the data in NOW. Also, an east-west gradient in low cloud appears such that the frequency of observation increases from NEW to SLIP, with extensive periods of overcast sky in the Beaufort and Bering Seas. Although many of these differences in cloud form and base height are rooted in the larger scale dynamical flow, it has been shown in the NOW region that topography and wind direction may influence cloud morphologies downstream of the survey area.

In terms of parameterizing these clouds, no single short- or longwave parameterization was applicable to all polynyas with minimal error. The Moritz (1978) shortwave equation was favored in all but NOW99 and SLIP99, the only data sets collected during seasonal transitions; however, its error only achieved acceptable levels ($< 2\ W \cdot m^{-2}$) in BFL. Longwave schematic preferences were more evenly distributed, though the difference in the equation structure is too small to warrant mention.

After performing several sensitivity tests with varying aerosol load, solar geometry, and sorting efficiency, the surface albedo was identified as an influential parameter to surface radiative flux, and consequently, cloud forcing calculations. Differences in reflected shortwave radiation spanned several orders of magnitude depending upon the surface classification, solar zenith angle, and prescribed albedo. These Arctic surface albedos change over very short spatial scales as ice cover breaks up during the summer, replacing a high (> 50%) albedo frozen surface with a low albedo (< 10%) water surface. The albedo of the snow-covered ice also undergoes rapid reduction as the snow begins to melt, and significant changes can occur on timescales of hours. Thus it is clear that for improvements in modeling of cloud forcing to be made, significant attention must be directed towards achieving realistic representations of surface albedo.

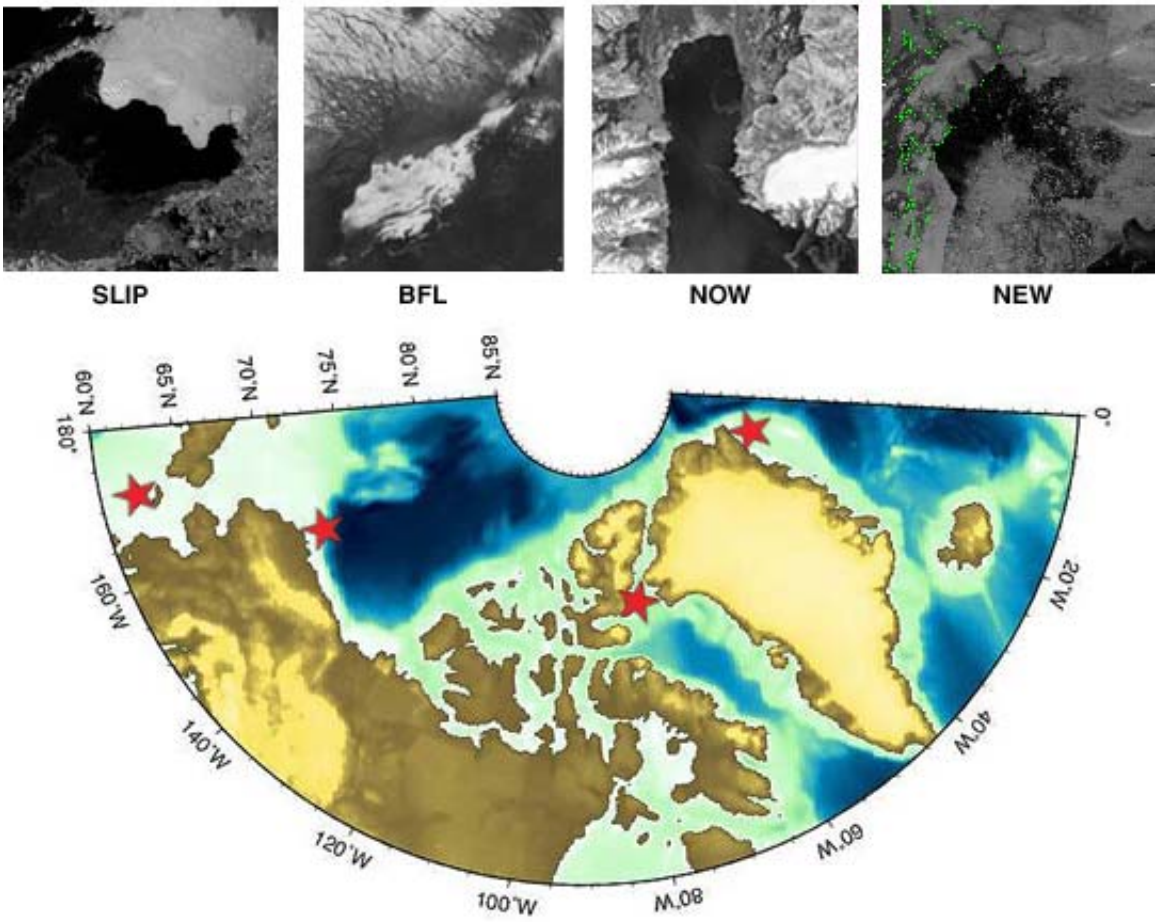

Figure 1. Bathymmetric map of the North American Arctic. Red stars indicate positions of four polynyas analyzed in this study. They are, from east to west, the NEW (Northeast Water), NOW (North Water), BFL (Barrow Flaw Lead), and SLIP (St. Lawrence Island Polynya).

4. REFERENCES

Chen, T., W.B. Rossow, and Y. Zhang, 2000, Radiative effects of cloud-type variations, *J. Climate*, **13**, 264-286.

Curry, J.A. And E.E. Ebert, 1992, Annual cycle of radiation fluxes over the Arctic Ocean: sensitivity to cloud optical properties, *J. Climate*, **5**, 1267-1280.

Curry, J.A., W.B. Rossow, D. Randall, and J.L. Schramm, 1996, Overview of Arctic cloud and radiation characteristics, *J. Climate*, **9**, 1731-1764.

Curry, J.A., J.L. Schramm, and E.E. Ebert, 1993, Impact of clouds on the surface radiation balance of the Arctic Ocean, *Meteor. And Atmos. Phys.*, **51**, 197-217.

Han, W. and K. Stamnes, 1999, Remote sensing of surface and cloud properties in the Arctic from AVHRR measurements, *J. Applied Meteor.*, **38**, 989-1012.

Hobbs, P.V., A.L. Rangno, M. Shupe, and T. Uttal, 2001, Airborne studies of cloud structures over the Arctic Ocean and comparisons with retrievals from ship-based remote sensing measurements, *J. Geophys. Res.*, **106**, 15029-15044.

Key, J., and A.J. Schweiger, 1998, Tools for atmospheric radiative transfer: Streamer and FluxNet, *Comput. and Geosci.*, **24**, 443-451.

Maslanik, J.A., J. Key, C.W. Fowler, T. Nguyen, and X. Wang, 2001, Spatial and temporal variability of satellite-derived cloud and surface characteristics during FIRE-ACE, *J. Geophys Res.*, **106**, 15233-15249.

Minnett, P.J., 1999, The influence of solar zenith angle and cloud type on cloud radiative forcing at the surface in the Arctic, *J. Climate*, **12**, 147-158.

Moritz, R.E., 1978, A model for estimating global solar radiation, Energy budget study in relation to fast-ice breakup processes in Davis Strait, R.G. Barry and J.D. Jacobs, eds., Occasional Paper 26, pp, 121-142, Inst. of Arctic and Alpine Res., Univ. of Colo., Boulder.

Ramanathan, V., R.D. Cess, E.F. Harrison, P. Minnis, B.R. Barkstrom, E. Ahmad, and D. Hartmann, 1989, Cloud-radiative forcing and climate: results from the Earth Radiation Budget Experiment, *Science*, **243**, 57-63.

Schweiger, A.J. And J.R. Key, 1992, Arctic cloudiness: comparison of ISCCP-C2 and Nimbus-7 satellite-derived coud products with surface-based cloud climatology, *J. Climate*, **5**, 1514-1527.

Warren, S.G., C.J. Hahn, J London, R.M. Chervin, and R. Jenne, 1988, Global distribution of total cloud cover and cloud type amounts over the ocean. NCAR Tech. Note TN-317+STR.

Figure 2. Streamer model sensitivity to variations in surface cover over a range of solar zenith angles. The scene description for each curve in the figure is listed below, in order from top to bottom.

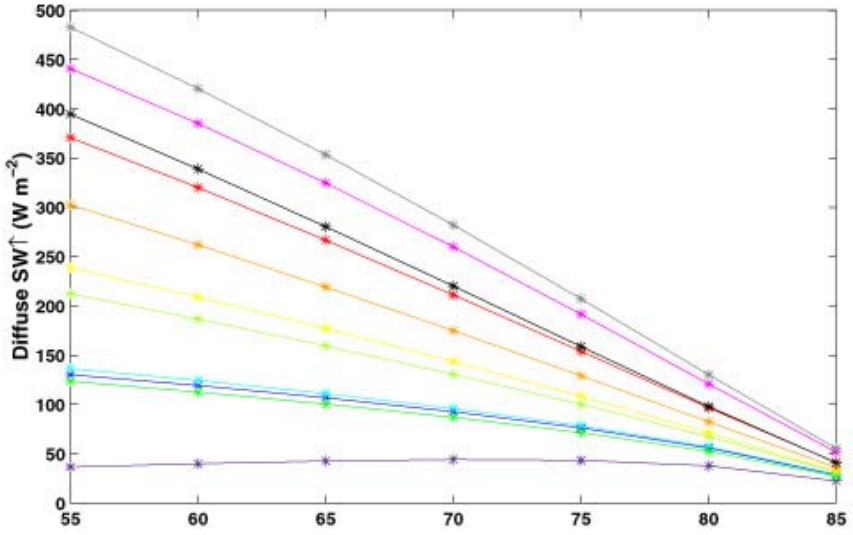

* **100% Fresh Snow**
* **100% Melting Snow**
* **100% Bare Ice**
* **10% Open Water, 15% Fresh Snow, 75% Bare Ice**
* **25% Open Water, 75% Bare Ice**
* **35% Open Water, 15% Meltponds, 15% Melting Snow, 35% Bare Ice**
* **50% Open Water, 50% Bare Ice**
* **75% Open Water, 15% Fresh Snow, 10% Bare Ice**
* **75% Open Water, 15% Melting Snow, 10% Bare Ice**
* **75% Open Water, 25% Bare Ice**
* **100% Open Water**